論文 / 著書情報
Article / Book Information

Title	Design of thin multilayer absorbers of graphite/polymer composites for W-band millimeter wave
Author	Tomoya Momose, Hirofumi Kondo, Masamitsu Haemori, Kotaro Kajikawa
Citation	Japanese Journal of Applied Physics, Vol. 64, , 022003
Pub. date	2025, 2
DOI	http://dx.doi.org/10.35848/1347-4065/adac21
Creative Commons	Information is in the article.

Japanese Journal of
Applied Physics

REGULAR PAPER • OPEN ACCESS

Design of thin multilayer absorbers of graphite/polymer composites for W-band millimeter waves

To cite this article: Tomoya Momose *et al* 2025 *Jpn. J. Appl. Phys.* **64** 022003

OPEN ACCESS

Japanese Journal of Applied Physics **64**, 022003 (2025) **REGULAR PAPER**

https://doi.org/**10.35848/1347-4065/adac21**

Design of thin multilayer absorbers of graphite/polymer composites for W-band millimeter waves

Tomoya Momose[1], Hirofumi Kondo[2], Masamitsu Haemori[2], and Kotaro Kajikawa[1*]

[1]*Department of Electrical and Electronic Engineering, School of Engineering, Institute of Science Tokyo, Nagatsuta, Midori-ku, Yokohama 226-8501, Japan*

[2]*Advanced Technology Research Laboratories, Idemitsu Kosan Co., Ltd., 1280 Kamiizumi, Sodegaura, Chiba, 299-0267, Japan*

[*]E-mail: kajikawa@ee.e.titech.ac.jp

Received November 19, 2024; revised January 10, 2025; accepted January 19, 2025; published online February 10, 2025

Thin film absorbers with high performance for millimeter electromagnetic waves are designed using a genetic algorithm. The absorber is a graphite-dispersed siloxane composite multilayer with specific graphite contents. The designed absorber with a thickness of 0.3 mm exhibits an absorptance of more than 20 dB (99%) in the automotive radar frequency band (76 – 81 GHz), and that with a thickness of 0.5 mm exhibits a broadband absorptance of more than 20 dB over the W-band (75–110 GHz). These films can contribute to the stable operation of advanced driver assistance systems. © 2025 The Author(s). Published on behalf of The Japan Society of Applied Physics by IOP Publishing Ltd

Supplementary material for this article is available online

1. Introduction

Advanced driver assistance systems (ADAS) have been introduced to ensure the safety of drivers, passengers, and other road users. Adaptive cruise control and collision avoidance operate in the 76–77 GHz band, whereas blind spot detection and lane change assist utilize the 77–81 GHz band. Previous studies have simulated signal propagation between the radar sensors of vehicles on highways, demonstrating that multiple signals can reach the receivers.[1)] Accordingly, interference may occur, resulting in the generation of ghost targets and reducing the signal-to-noise ratio. This can negatively affect the ADAS performance. The use of higher frequency bands beyond the current radar bands has also been expected to improve angular resolution and precision and reduce antenna size.[2)]

Microwave absorbers have been developed to achieve both thinness and broadband absorption. However, previously proposed absorbers have had difficulty balancing these requirements.[3)] A radar absorber, composed of a resistive square-patch frequency-selective surface and prepared using screen printing, demonstrated an absorptance exceeding 20 dB (99%) in the 75–82 GHz band.[4)] Its high-resolution surface patterns and precise thickness requirements make it unsuitable for mass production. A 1 mm-thick graphene foam absorber provided broadband absorptance exceeding 90% across the 7–18, 27–40, and 75–110 GHz bands.[5)] It was fabricated using complex processes. Although the absorbers with such complex structures are thin and have absorption bands suitable for specific applications, the manufacturing complexity and difficulty of large-area production make them impractical. Thus, absorbers with multiple layers can be used to develop broadband absorbers.[6–9)] Additionally, graphene has high electrical conductivity and low weight, enabling us to develop extremely thin and lightweight absorbers.[5,10–12)] Thus, a multilayer structure composed of graphite/polymer composite can simultaneously achieve broadband absorption, thinness, and lightness.

In this study, we designed a highly absorptive, thin, and practically manufacturable multilayer absorber (MLA) of graphite-dispersed polydimethylsiloxane (PDMS) for automotive radar applications. Graphite was used as a material for absorbing millimeter waves. PDMS, which has good dispersibility for graphite, was used as a host material.

To design such an MLA, we must determine many unknown parameters. Machine learning using neural networks is one of the most powerful tools for solving this type of problem. However, it requires extensive datasets, which are unrealistic to prepare.[13)] Instead, we employed a genetic algorithm (GA).[14)] This approach is an effective strategy for determining many parameters for optimization.[15–19)] In this study, we investigated two types of MLAs: a narrowband MLA for the automotive radar frequency (ARF) band (76–81 GHz) and a broadband MLA covering the W-band (75–110 GHz). The latter is expected to be utilized in future applications. The objective was to design an MLA with an absorptance of 20 dB or more for each band. Both types of absorbers were successfully optimized.

2. Methods

Figure 1(a) shows a schematic of the composite material in which graphite was dispersed in PDMS used as a matrix. The permittivity of graphite was evaluated experimentally. The details of the evaluation are described in Supplementary Data S1. Figure 1(b) shows an overview of the 10 layer MLA on an ideal metal substrate, the permittivity of which was set at –10000. The layers are numbered starting from the layer facing free space. The thickness of layer i is denoted as d_i, and the total thickness of the MLA is D. The electromagnetic wave is incident normally; therefore, no polarization dependence occurs.

We used a GA with the value encoding scheme to design the MLA.[14)] This approach is practical when the objective function is a black box or a multimodal function that cannot be solved using mathematical programming and when a reasonably good solution must be obtained within a realistic

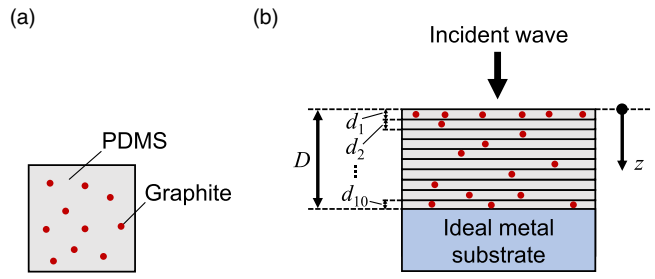

Fig. 1. Schematic of MLAs. (a) Thin film of graphite and PDMS. (b) 10 layer MLA on an ideal metal. D is the total thickness of the MLA, and d_i is the thickness of layer i. The z axis is defined as the surface normal direction.

time frame. In the GA calculation, we set the thickness of each layer to be the same. The graphite weight content f_i, where i is the number of layers ($i = 1 - 10$), was determined using the GA. The graphite content was restricted to $0\% - 10\%$ (10% restriction) or $0\% - 15\%$ (15% restriction), ensuring uniform graphite dispersion within the matrix. We investigated different total thicknesses D of the MLA, with $D =$ 0.1, 0.2, 0.3, 0.4, and 0.5 mm. Subsequently, the thickness of each layer was $D/10$ mm.

The transfer matrix method was adopted to evaluate the reflectance R.[20] The absorptance A in dB was calculated using the following equation because an ideal metal substrate was used:

$$A = -10\log_{10} R. \tag{1}$$

The fitness function (F) was set to provide an absorptance of over 20 dB covering both the ARF band (76–81 GHz) and W-band (75–110 GHz), as follows:

$$\begin{aligned} F = &\int_{75\,\mathrm{GHz}}^{76\,\mathrm{GHz}} \min(A(f), 20)\, df \\ &+ \int_{76\,\mathrm{GHz}}^{81\,\mathrm{GHz}} 1000 \cdot \min(A(f), 20)\, df \\ &+ \int_{81\,\mathrm{GHz}}^{110\,\mathrm{GHz}} \min(A(f), 20)\, df \end{aligned} \tag{2}$$

This fitness function emphasizes broadband absorption while reducing sharp absorption peaks. To de-emphasize candidates with sharp absorption peaks, we introduced a capped absorptance, $\min(A(f), 20)$. The min operator selects the smaller of the two given values. To ensure absorption peaks in the ARF band ($76 - 81$ GHz), we weighted the absorptance in this range by 1000. The designed results using a simpler F are provided in Supplementary Data S2, in which successful results were not obtained. This indicates that Eq. (2), which uses the capped function, is essential. GA calculations were performed to determine the graphite content for each layer that yielded the highest F. The Distributed Evolutionary Algorithms in Python (DEAP) framework was used under the following conditions:[21] tournament selection size of 3, two-point crossover probability of $50\% - 90\%$, mutation probability of $20\% - 90\%$, a population size of 10000, and 200 generations. For each MLA thickness, 10 trials were conducted with varying pseudorandom numbers. The crossover and mutation probabilities were treated as variables to enhance evaluation efficiency, and further details are provided in the Supplementary Material of our previous paper.[13]

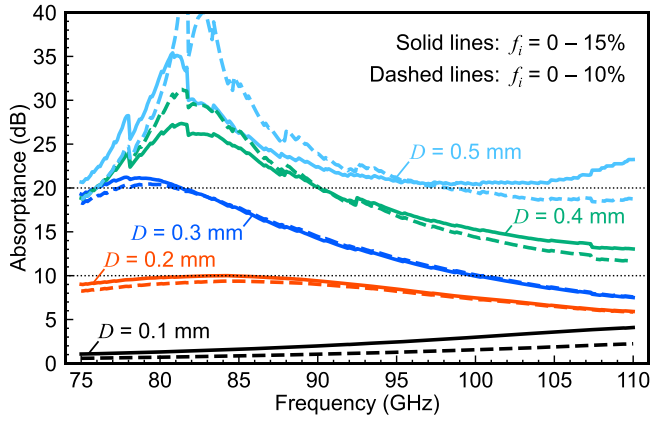

Fig. 2. Calculated absorptance for various absorber thicknesses D ranging from 0.1 to 0.5 mm. Solid lines represent cases with a graphite content limit of 15%, and dashed lines correspond to a limit of 10%.

3. Results and discussion

3.1. Absorptance spectra

Figure 2 shows the absorptance of the MLAs with a total thickness of $D = 0.1 - 0.5$ mm in the W-band. The solid lines represent the absorptance spectra of the MLA designed under the 15% restriction, whereas the dashed lines represent those under the 10% restriction. As the total thickness D increased, greater absorptance existed across the entire W-band. The MLA with $D = 0.2$ mm (solid red line) had approximately an absorptance of 10 dB in the ARF band ($76 - 81$ GHz). This did not satisfy the requirement for an absorptance of 20 dB or higher. In contrast, the MLA with $D = 0.3$ mm (solid blue line) exceeded 20 dB. The MLA with $D = 0.5$ mm (solid light blue line) had an absorptance higher than 20 dB across the entire W-band. Even under the 10% restriction, the GA-designed MLAs exhibited a similar absorption performance.

Figure 3 shows the graphite content profiles designed under the 15% restriction. The MLA with $D = 0.1$ mm showed that all 10 layers had a maximum content of 15%, indicating that the MLA was homogeneous. In the MLAs with $D = 0.2$ and 0.3 mm, the layers with a high graphite content were designed to be on the side facing the air, and the graphite in the other layers was negligible. In contrast, in the MLAs with $D = 0.4$ and 0.5 mm, the layers with a high graphite content were designed to be on the side facing the metal substrate. Figure 4 shows the graphite content profiles designed under the 10% restriction. The trends were similar to those designed under the 15% restriction.

3.2. Narrowband simplified MLA

When manufacturing MLAs, a structure with fewer layers is preferable. Here, we show that a high-performance MLA can be achieved without losing its absorption characteristics even when the number of layers is reduced. The reduced structure is considered based on the design determined using a GA.

As shown in Fig. 3(c), the graphite contents of the MLA at $D = 0.3$ mm were approximately 15% and 3% for the first and second layers, respectively. In contrast, the graphite contents of the third to tenth layers were nearly zero. This is because the electric field in the graphite-free layers was weak, as shown in Fig. 5(a), in which the calculated electric field, E, normalized by the incident field, E_0, is plotted. Regarding this structure, we designed a two-layer simplified MLA, in which the outermost layer facing the air contained graphite, and the

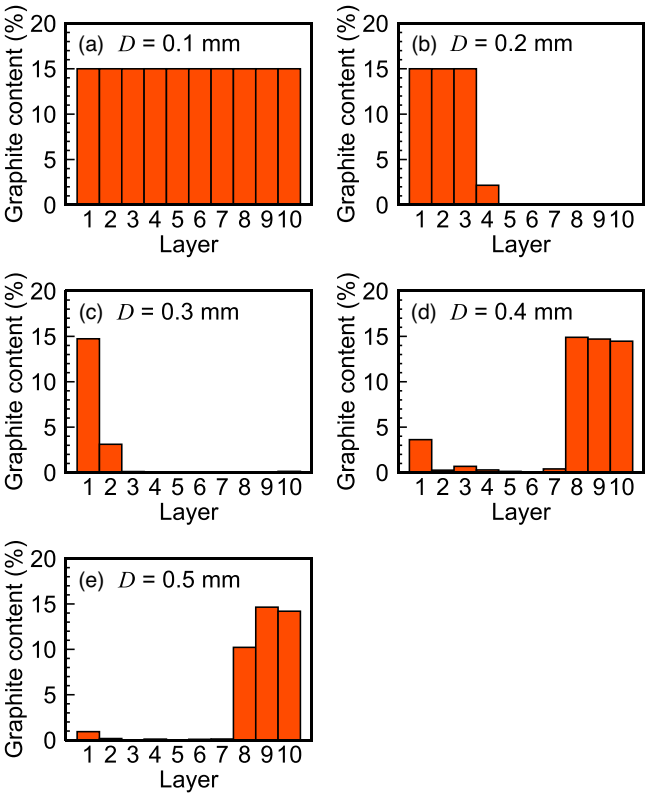

Fig. 3. Graphite content profiles for MLAs with different total thicknesses D, designed using GA under the 15% restriction.

spacer layer was sandwiched by the outermost layer and metal substrate. We comprehensively investigated the thickness of each layer to maximize the fitness function. (Details are given in the Supplementary Data S3.1) We observed that

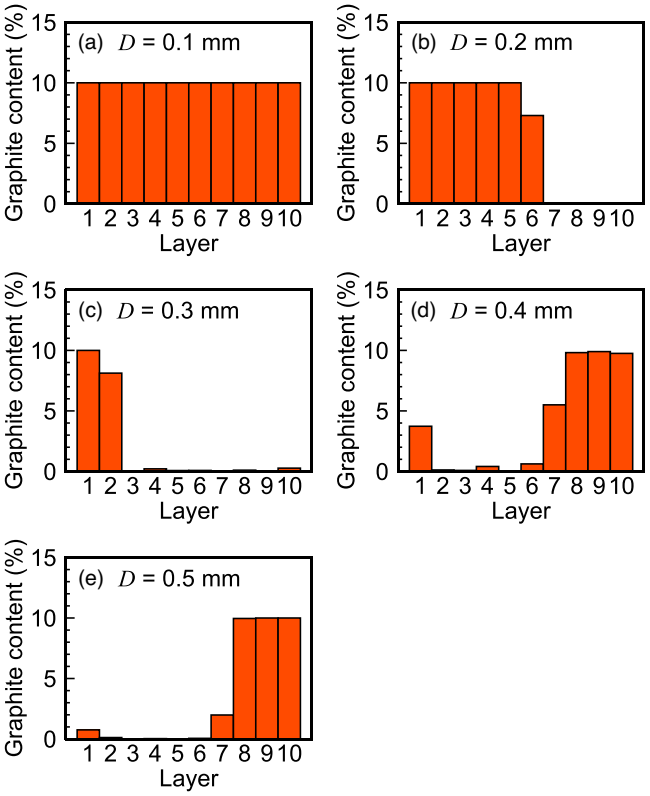

Fig. 4. Graphite content profiles for MLAs with different total thicknesses D, designed using GA under the 10% restriction.

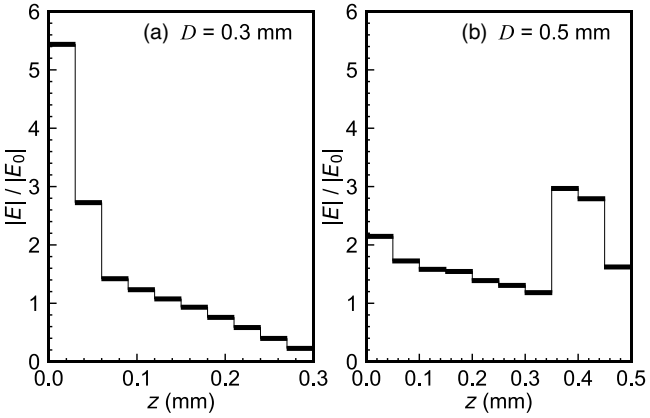

Fig. 5. Normalized electric field distribution in (a) the narrowband MLA (D = 0.3 mm) and (b) the broadband MLA (D = 0.5 mm).

the two-layer MLA also exhibited high performance, and its absorptance spectrum is shown in Fig. 6. The determined MLA structure is shown in the inset. The spectrum of a 10 layer MLA optimized using GA is shown with a dashed line for comparison. They were almost identical and achieved the target of having an absorptance of over 20 dB in the ARF band at a total thickness of 0.3 mm.

The narrowband MLA can be compared with the concept of the Salisbury screen,[22] which comprises two layers: an absorption layer in the first layer and a lossless dielectric layer in the second layer, used as a spacer. The thickness of the lossless spacer layer, t, is

$$t = \frac{\lambda}{4n} \tag{3}$$

Here, λ is the peak wavelength in a vacuum, and n is the refractive index of the lossless dielectric spacer. The calculated thickness, t, at 78 GHz is 0.57 mm, whereas the thickness of the spacer layer is 0.26 mm, which does not match t. This is because the absorption layer is not thin, and the real part of the permittivity of the absorption layer exists.[23,24]

Table I compares the performance of various reported narrowband ARF absorbers. The candidates cover most of the ARF band (76–81 GHz). Although our MLA has a similar absorptance to the resistive square-patch frequency-

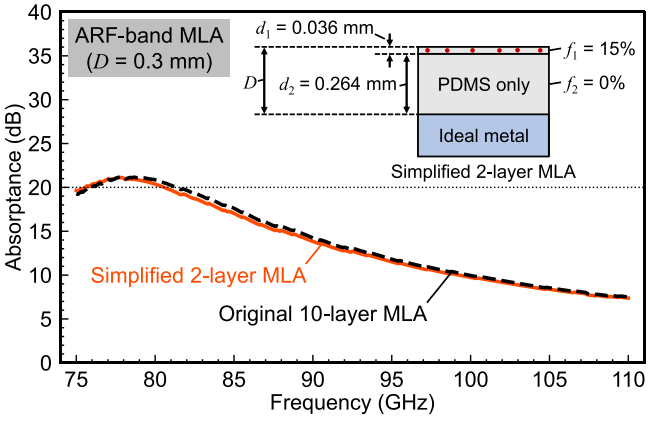

Fig. 6. Comparison of the original and simplified graphite contents designs for an absorber thickness of D = 0.3 mm, calculated under the 15% restriction. The schematic of the simplified two-layer MLA is depicted in the inset.

Table I. Performance comparison of narrowband ARF absorbers.

Frequency range (GHz)	Absorptance (%)	Thickness (mm)	Method	References
75 – 82	> 99	0.5	Fabrication	4
75 – 80	> 80	0.126	Fabrication	25
76 – 81	> 99	0.3	Simulation	This work

Table II. Performance comparison of broadband absorbers.

Frequency range (GHz)	Absorptance (%)	Thickness (mm)	Method	References
38 – 142	> 90	1	Simulation	27
50 – 460	> 90	1	Simulation	28
73.5 – 110	> 90	0.526	Fabrication	30
75 – 110	> 90	1	Fabrication	5
39.2 – 200	> 95	0.74	Simulation	12
50 – 300	> 90	1	Simulation	29
75 – 110	> 99	0.5	Simulation	This work

selective surface reported by Kim et al.,[4] and is thinner than theirs. The absorber, reported by Singh et al., is thinner[25] but does not achieve sufficient absorptance. Both absorbers are fabricated from metasurfaces, which require complex manufacturing processes. In contrast, our MLA does not require surface patterning and is thinner than the conventional Salisbury screen.

3.3. Broadband simplified MLA

The broadband MLA was also simplified as we did for the narrowband MLA. For the broadband MLA, the GA provides a structure in which a high graphite-content layer is located on the metal substrate side, a low graphite-content layer is located at the outermost layer on the air side, and a spacer layer with negligible graphite content is sandwiched between them, as shown in Figs. 3(d) and 3(e). The electric field profile for $D = 0.5$ mm is shown in Fig. 5(b). This graphite-content profile can be explained by the electric field distribution. The electric field is higher near the metal substrate and electromagnetic waves can be efficiently absorbed by placing the absorption layer here.

Similar to the narrowband MLA design, we comprehensively surveyed the thickness of each layer. Details are given in Supplementary Data S3.2. We observed a three-layer MLA structure that exhibited a high performance. The absorptance spectrum is shown in Fig. 7. For comparison, the spectrum of the ten-layer MLA optimized using the GA is shown as a dashed line. Although the three-layer simplified MLA has slightly inferior absorption characteristics, it still satisfies the target of an absorptance of over 20 dB in the W-band at a total thickness of 0.5 mm. The spectrum of MLA with the graphite removed from the outermost layer ($f_1 = 0\%$) is shown as a blue line. This spectrum does not satisfy the requirements, indicating that the first outermost layer must have graphite even at low content. The absorptive layers adjacent to the substrate and the first lossy layer enable us to conduct the MLA with absorptance over 20 dB across the entire W-band.[26]

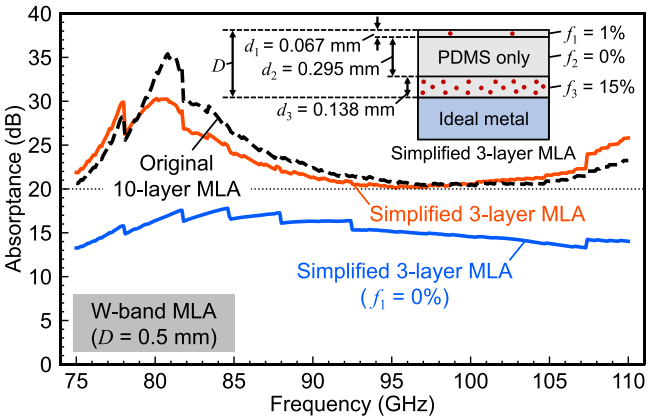

Fig. 7. Comparison of the original and simplified graphite contents designs for an absorber thickness of $D = 0.5$ mm, calculated under the 15% restriction. The schematic of the simplified three-layer MLA is depicted in the inset. The stair-shaped spectra are due to the permittivity of PDMS measured in two significant digits.

Table II compares the performances of broadband absorbers reported in other studies. All absorbers cover the W-band. The 3D metamaterial,[27,28] graphene frequency-selective surface,[12] and the multilayer absorber created from PMMA and graphene[29] have only been reported through simulations and have not been fabricated. Wu et al.[30] reported an absorber of an Ag mesh using the electrohydrodynamics (EHD) printing method. Their absorber is as thin as ours, but the absorptance (>90%) is lower than ours. In addition, the EHD printing speed is slow[31] and unsuitable for large-area production. The absorber reported by Zhang et al.[5] is thick, and the absorptance is much lower than our MLA's. Our absorber exhibits the highest absorptance (over 99%) and is the thinnest ($D = 0.5$ mm). In addition, it can be fabricated with a simple process and is scalable for large areas.

4. Conclusion

We successfully designed two MLAs with the desired performance using a GA: an absorptance of more than 20 dB over the ARF band or W-band. The necessary thickness of the narrowband MLA covering the ARF band is 0.3 mm, and that of the broadband MLA covering the W-band is 0.5 mm. They are the thinnest among other absorbers, with an absorptance of more than 20 dB. In the GA design, the MLA consists of 10 layers. However, MLAs with fewer layers are preferred for actual production. Therefore, we attempted to simplify the structure and found the MLAs with a few layers with the same performance. This paper shows that the GA can be used to design structures with the highest performance under specified conditions. Our absorbers can aid in reducing false detections in high-traffic radar applications for ADAS and autonomous driving technologies.

Acknowledgments

This work was partly supported by JST SPRING, Japan Grant No. JPMJSP2106 and JPMJSP2180.

ORCID iDs

Tomoya Momose https://orcid.org/0009-0009-1720-1080
Kotaro Kajikawa https://orcid.org/0000-0002-3135-8887

1) C. Waldschmidt, J. Hasch, and W. Menzel, IEEE J. Microw. **1**, 135 (2021).
2) M. Köhler, J. Hasch, H. L. Blöcher, and L. P. Schmidt, Int. J. Microw. Wirel. Technol. **5**, 49 (2013).
3) A. Choudhary, S. Pal, and G. Sarkhel, Int. J. Microw. Wirel. Technol. **15**, 347 (2023).
4) M. S. Kim and S. S. Kim, IEEE Microw. Wirel. Lett **29**, 779 (2019).
5) Y. Zhang, Y. Huang, T. Zhang, H. Chang, P. Xiao, H. Chen, Z. Huang, and Y. Chen, Adv. Mater. **27**, 2049 (2015).
6) J. Sun, L. Liu, G. Dong, and J. Zhou, Opt. Express **19**, 21155 (2011).
7) M. Amin, M. Farhat, and H. BaÄŸci, Opt. Express **21**, 29938 (2013).
8) F. G. Garakani, G. Moradi, and A. Ghorbani, Opt. Continuum **2**, 1158 (2023).
9) G. Xu, J. Zhang, X. Zang, O. Sugihara, H. Zhao, and B. Cai, Opt. Express **24**, 23177 (2016).
10) K. Batrakov, P. Kuzhir, S. Maksimenko, A. Paddubskaya, S. Voronovich, P. Lambin, T. Kaplas, and Y. Svirko, Sci. Rep. **4**, 7191 (2014).
11) K. Batrakov, P. Kuzhir, S. Maksimenko, N. Volynets, S. Voronovich, A. Paddubskaya, G. Valusis, T. Kaplas, Y. Svirko, and P. Lambin, Appl. Phys. Lett. **21**, 123101 (2016).
12) D. K. Zhu, Y. S. Li, W. Y. Yin, and E. P. Li, "A transparent broadband absorber based on graphene," Asia-Pacific Int. Symp. on Electromagnetic Compatibility (APEMC 2016) (Shenzhen), 2016, 1025, 10.1109/APEMC.2016.7522935.
13) T. Momose, M. Toma, and K. Kajikawa, J. Opt. Soc. Am. B **41**, 1815 (2024).
14) S. Katoch, S. Chauhan, and V. Kumar, Multimed. Tools Appl. **80**, 8091 (2021).
15) S. Liu, Z. Ye, R. Tan, M. Han, H. Zhuang, and P. Chen, Opt. Express **32**, 30969 (2024).
16) Z. Yu, Y. Feng, X. Xu, J. Zhao, and T. Jiang, J. Phys. D **44**, 185102 (2011).
17) A. Mirzaei, A. E. Miroshnichenko, I. V. Shadrivov, and Y. S. Kivshar, Sci. Rep. **5**, 9574 (2015).
18) Y. Han, W. Che, C. Christopoulos, Y. Xiong, and Y. Chang, IEEE Trans. Electromagn. Compat. **58**, 747 (2016).
19) S. Chakravarty, R. Mittra, and N. R. Williams, IEEE Trans. Microw. Theory Techn. **49**, 1050 (2001).
20) D. S. Bethune, J. Opt. Soc. Am. B **6**, 910 (1989).
21) F. A. Fortin, F. M. D. Rainville, M. A. Gardner, M. Parizeau, and C. Gagné, J. Mach. Learn. Res. **13**, 2171 (2012).
22) R. L. Fante and M. T. McCormack, IEEE Trans. Antennas Propag. **36**, 1443 (1988).
23) P. G. Lederer, "Modelling of practical Salisbury screen absorbers," IEE Colloq. on Low Profile Absorbers and Scatterers (London, UK) 1/1 (1992).
24) J. Kim, "Design of Salisbury screen absorbers using dielectric lossy sheets," IEEE Int. Conf. on Microwave Technology & Computational Electromagnetics, 22-25 May 2011 (Beijing, China), 17, 10.1109/ICMTCE.2011.5915154.
25) P. K. Singh, K. A. Korolev, M. N. Afsar, and S. Sonkusale, Appl. Phys. Lett. **99**, 264101 (2011).
26) F. Li, P. Chen, Y. Poo, and R. X. Wu, "Achieving perfect absorption by the combination of Dallenbach layer and Salisbury screen," 2018 Asia-Pacific Microwave Conf. (APMC), Kyoto, Japan, 1507, 10.23919/APMC.2018.8617477.
27) X. Ling, Z. Xiao, X. Zheng, J. Tang, and K. Xu, J. Electromag. Waves Appl. **30**, 2325 (2016).
28) A. Vahidi, H. Rajabalipanah, A. Abdolali, and A. Cheldavi, Appl. Phys. A **124**, 337 (2018).
29) D. Mencarelli, L. Pierantoni, M. Stocchi, and S. Bellucci, Appl. Phys. Lett. **109**, 093103 (2016).
30) Y. Wu, C. Fu, S. Qian, Z. Zong, X. Wu, Y. Yue, and W. Gu, IEEE Antennas Wirel. Propag. Lett. **19**, 1345 (2020).
31) Y. Wu, Y. Deng, J. Wang, Z. Zong, X. Chen, and W. Gu, IEEE Trans. Terahertz Sci. and Technol **9**, 637 (2019).